Widespread seismicity excitation throughout central Japan following the 2011 M=9.0 Tohoku earthquake, and its interpretation by Coulomb stress transfer

Shinji Toda[1], Ross S. Stein[2], Jian Lin[3]

[1]Disaster Prevention Research Institute, Kyoto University, Japan
[2]U.S. Geological Survey, Menlo Park, California, USA
[3]Woods Hole Oceanographic Institution, Woods Hole, Massachusetts, USA

Plain English Summary

We report on a broad and unprecedented increase in seismicity rate for microearthquakes (M≥2) over a broad 600 by 200 km (360 by 120 mi) area across inland Japan, parts of the Japan Sea and the Izu islands, following the M=9.0 Tohoku mainshock. The seismicity increase occurs at distances of up to 425 km (360 mi) from the region of high (≥15 m or 50 ft) seismic slip on the megathrust rupture surface of the M=9 earthquake. Are these aftershocks, and if so what do they signify for the likelihood of large earthquakes across this region? While the origin and implications of the seismicity increase is subject to debate, its occurrence is beyond dispute. It was not seen for the 2004 M=9.1 Sumatra and 2010 M=8.8 Chile earthquakes, but they lacked the seismic networks necessary to detect such small events. Here we explore the possibility that the rate changes are the product of static or permanent stress transfer from the mainshock to small surrounding faults. We find that half of the areas we can examine show a positive association between calculated stress changes and the observed seismicity rate change, three show a negative association, and in four show changes too small to assess. Regardless of the process that promotes the aftershocks, we argue that the microseismicity increases demonstrate that the 'remote' inland Japan and Japan Sea and shocks (e.g., the Nagano Mw=6.3 on 3/12 03:59, the Japan Sea Mw=6.2 on 3/12 04:46, the Mt. Fuji Mw=5.8 on 3/15, 22:31) are not exceptional; in fact they are not truly isolated events. Instead, they simply represent the largest shocks in a very broad zone of elevated seismicity rate that is evident for M≥2 earthquakes.

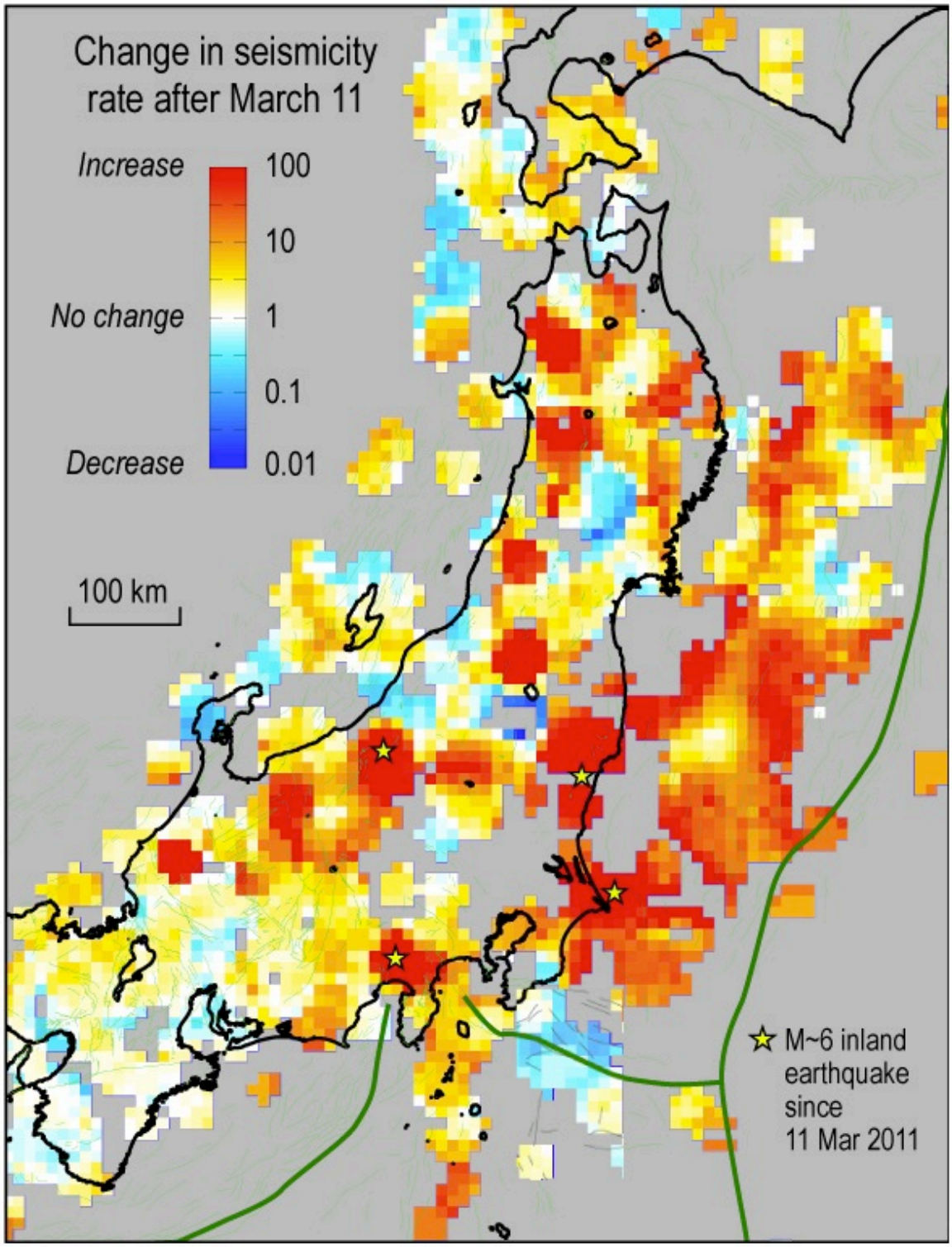
Change in seismicity rate after March 11
Increase
No change
Decrease
100
10
1
0.1
0.01
100 km
M~6 inland earthquake since 11 Mar 2011

Widespread seismicity excitation throughout central Japan following the 2011 M=9.0 Tohoku earthquake, and its interpretation by Coulomb stress transfer

Shinji Toda[1], Ross S. Stein[2], Jian Lin[3]

[1]Disaster Prevention Research Institute, Kyoto University, Kyoto, Japan

[2]U.S. Geological Survey, Menlo Park, California, USA

[3]Woods Hole Oceanographic Institution, Woods Hole, Masachussetts, USA

We report on a broad and unprecedented increase in seismicity rate following the M=9.0 Tohoku mainshock for M≥2 earthquakes over inland Japan, parts of the Japan Sea and Izu islands, at distances of up to 425 km from the locus of high (≥15 m) seismic slip on the megathrust. Such an increase was not seen for the 2004 M=9.1 Sumatra and 2010 M=8.8 Chile earthquakes, but they lacked the seismic networks necessary to detect such small events. Here we explore the possibility that the rate changes are the product of static Coulomb stress transfer to small faults. We use the nodal planes of M≥3.5 earthquakes as proxies for such small active faults, and find that of fourteen regions averaging ~80 by 80 km in size, half show a positive association between calculated stress changes and the observed seismicity rate change, three show a negative correlation, and four show changes too small to assess. This work demonstrates that seismicity can turn on in the nominal stress shadow of a mainshock as long as small geometrically diverse active faults exist there, which is likely quite common.

1. Introduction

The M=9.0 Tohoku-chiho Taiheiyo (hereafter, 'Tohoku') earthquake resulted from slip on a roughly 500-km-long and 200-km-wide seismic megathrust source (e.g., *Wei et al*., 2011). Many offshore aftershocks, including four M≥7 and ~70 M≥6 shocks, have struck during the ensuing three weeks. The possibility of other large earthquakes on adjacent portions of the megathrust, similar to the 28 March 2005 Mw=8.6 Simeulue-Nias earthquake following the 26 December 2004 Mw=9.1 Sumatra-Andaman earthquake [*Nalbant et al.,* 2005; *Pollitz et al.,* 2006] are thus possible. Sites of potential tsunamigenic earthquakes include the Sanriku-Hokubu area to the north, and Off-Boso (east of the Boso peninsula) to the south (Headquarters for Earthquake Research Promotion, 2005) of the 2010 Tohoku rupture.

Equally important for the exposed population and infrastructure would be the occurrence of large inland shocks in northern Honshu. Three M~6 shallow inland earthquakes have already struck as far as ~300 km from the M=9 source within five days of the Tohoku mainshock, reaffirming the broad reach and triggering potential of the great quake. Among such inland sites, none is more important than Tokyo, which was last struck by the 1923 Kanto M=7.9 Sagami megathrust event [*Nyst et al.,* 2006], and a deeper inland event in the 1855 M~7.2 Ansei-Edo earthquake [*Grunewald and Stein,* 2006]. This concern is heightened by several inland large earthquakes in Tohoku that have followed M=7-8 interplate events by months to a decade [*Shimazaki*, 1978; *Seno*, 1979; *Churei*, 2002], including the 31 August 1896 Mj=7.2 Rikuu earthquake, which produced a 30-km-long surface rupture that devastated the eastern Akita Prefecture (with 200 deaths).

To evaluate the potential triggering impact of the Tohoku earthquake to inland Japan, we analyze the seismicity rate change since the Tohoku mainshock, and calculate the associated static Coulomb stress changes over the region of seismicity rate change.

2. Inland Seismicity Rate Changes Associated with the Tohoku Earthquake

The widespread seismicity rate increase across central Japan and extending west to the Japan Sea and south to the Izu islands in evident in Figure 1. Broadly, there are strong increases in seismicity rate across a region extending up to 300 km from the distal edges of the M=9 rupture surface, and 425 km from the locus of high (≥15 m) seismic slip. In addition to the microseismicity, an Mj=6.7 earthquake occurred 13 hours after the Tohoku mainshock in box J, a Mj=6.4 earthquake occurred 24 hours after the Tohoku earthquake in box A, and a Mj=6.4 earthquake struck about 4.5 days after the Tohoku earthquake at the base of Mt. Fuji. While it might appear that these remote earthquakes are distinct from aftershocks closer to the rupture plane, Figure 1 suggests that it is more likely that they are simply the largest events to occur within the broad zone of increased seismicity rate.

The broad seismic excitation for Tohoku is unprecedented, although for the roughly-equivalent 2004 M=9.1 Sumatra, Indonesia, and 2010 M=8.8 Maule, Chile, earthquakes, no M<4.7 aftershock could be detected. Also, remote earthquake triggering was observed at even great distances but much lower densities following the 1992 M=7.3 Landers and 2002 M=7.9 Denali, earthquakes [*Hill*, 2008].

Sudden increases of post-Tohoku seismicity are observed in regions B (Akita), E (southern Fukushima – northern Ibaraki), F (Cape Inubou), H (Mt. Hotaka-Mt. Asahi), I (Kanto), where a burst of seismicity began at the head of Tokyo Bay several days after the Tohoku shock, M (Izu and islands), and K (Hida mountain range) (Figure 1). A possible increase in seismicity rate delayed by 1-3 days is observed in the box D. The increase in seismicity in regions J and A could be masked by aftershocks of the M~6 mainshocks, or the larger events could be part of the same process. The JMA (Japan Metetorological Agency) PDE catalog normally lists earthquakes that have occurred until two days before present, but because of the enormous number of aftershocks since March 11, human inspection of the records is incomplete (time series in Figure 1). Even during the first week after March 11,

77 data transfer interruptions caused by seismic station power outages and damage affect the
78 earthquake record, and thus apparent seismicity rate drops might be artifacts. In contrast,
79 sudden seismicity rate jumps are likely real. Some of the rate increases, such as boxes J and
80 M, exhibit gradual declines since March 11 reminiscent of aftershock sequences.
81
82 **3. Calculation of the Coulomb Stress Change**
83 The static Coulomb stress change caused by a mainshock has been widely applied to
84 assess areas of subsequent off-fault aftershocks (e.g., *Reasenberg and Simpson,* 1992). The
85 Coulomb stress change is defined as $\Delta CFF = \Delta\tau + \mu\Delta\sigma$, where τ is the shear stress on the fault
86 (positive in the inferred direction of slip), σ is the normal stress (positive for fault
87 unclamping), and μ is the apparent friction coefficient. Failure is promoted if ΔCFF is positive
88 and inhibited if negative; both increased shear and unclamping of faults are taken to promote
89 failure, with the influence of unclamping controlled by fault friction.
90 To resolve the Coulomb stress change on a 'receiver fault' (fault receiving stress from a
91 mainshock) requires a source model of the earthquake fault slip, as well as the geometry and
92 slip direction on the receiver. One can assume that the receiver faults share the same strike,
93 dip and rake as the mainshock source fault, one can resolve stress on a major fault of known
94 geometry (e.g., *McCloskey et al.,* 2003), or one can find the receiver faults at every point that
95 maximize the Coulomb stress increase given the earthquake stress change and the tectonic
96 stress [*King et al.,* 1994], termed the 'optimally-oriented' Coulomb stress change. However,
97 the M=9.0 Tohoku earthquake at least temporarily raised the seismicity rate across a region so
98 large that various types of faults and tectonic stress fields associated with the complex
99 convergence of three tectonic plates are intermingled. One solution is to resolve the stress
100 change on major active faults [*Toda et al.*, 2011, submitted] based on their inferred geometry
101 and slip sense. While this is instructive as a guide to the likelihood that one of these major
102 faults could rupture, the faulting mechanisms of small to moderate shocks that dominate the

103 local seismicity increase are undoubtedly more complex and varied than the associated major
104 structures, and so here we propose an alternative.
105
106 **4. Use of Focal Mechanisms as Proxies for Small Active Faults**
107 We instead resolve the Coulomb stress changes on the nodal planes of the abundant small
108 earthquakes as proxies for active faults. We make use of fault plane solutions of the full,
109 14-year-long F-net catalog [*NIED*, 2011], which for inland Japan principally includes shallow
110 crustal earthquakes of Mj≥3.5; this corresponds to source dimension ≥400 m [*Wells and*
111 *Coppersmith,* 1994]. As evident by comparing the mapped active faults (green lines) with the
112 focal mechanisms in Figures 2a and 3a, even though the mapped faults [*Research Group for*
113 *Active Faults in Japan*, 1991] often have sinuous and en echelon traces, the focal mechanisms
114 reveal even more complexity, such as strike-slip faults amid the mapped thrust faults of
115 Tohoku, or thrust mechanisms with a wide range of strikes at the site of the 2008 Mj=7.2
116 Iwate-Miyagi Nairiku earthquake (box C in Figure 2a).
117 In *Toda et al.* [2011, submitted] we tested six representative source models and three
118 friction values to determine the model producing the greatest gain in aftershock mechanisms
119 promoted by the mainshock relative to the background (pre-Tohoku) mechanisms. The *Wei et*
120 *al*. [2011] source model and a friction of 0.4 produces the greatest (62%) gain, and so we use
121 them here to calculate the stress changes in an elastic half space with Poisson's ratio 0.25 and
122 shear's modulus 3.2 x 10^5 bar, using Coulomb 3.2 (www.coulombstress.org). We resolve the
123 static Coulomb stress change on both nodal planes at each hypocenter because the normal
124 stress change is different on each plane in a set, and we do not know which of the two nodal
125 planes slipped. In Figs. 2b and 3b, we plot the maximum Coulomb stress change for the most
126 positive plane only (we would otherwise have to plot both sets of planes), and also place
127 positive changes (red dots) atop negative changes (blue dots) where earthquakes overlap.
128 Thus, the figures have an intentional 'red bias,' but Table 1 uses both nodal planes and has no

129 bias. We examine 14 rectangular areas where the seismicity is abundant (Figure 1) and where
130 focal mechanisms are available (Figs. 2a and 3a).
131
132 **5. Comparison of Seismicity Rate Changes and Coulomb Stress Changes**
133 Comparison of Figure 1 with Figures 2b and 3b indicates positive associations between
134 observed seismicity rate increases and Coulomb stress increases resolved on nodal planes in
135 seven of the 14 boxes. We find no clear changes in either seismicity rate or stress in 4 boxes,
136 and negative correlations, contradicting our hypothesis, in 3 boxes (Table 1).
137 The positive correlations include boxes F and I straddling the rupture, box M located
138 150-225 km from the rupture surface, and box K, 250 km from the rupture edge. In box I
139 (Kanto district), we included mechanisms as deep as 100 km because of the complex plate
140 configuration beneath Tokyo [*Toda et al*., 2008]. More than 80% of the stress changes for mid
141 to deeper shocks along the NS-trending 'Kanto seismic corridor' (box I) are positive.
142 There is also a correlation between the (albeit preliminary) seismicity rate decreases and
143 stress decreases in boxes C, G and L. Detecting seismicity rate decreases normally demands
144 not only a high rate of preceding seismicity, but also a long post-mainshock catalog that is not
145 yet available. Box C was the site of the 2008 Mj=7.2 Iwate-Miyagi Nairiku earthquake, and
146 box L was the site of the 2007 Mj=6.8 Noto Hanto earthquake; to be certain that these sites
147 sustained seismicity rate drops, one would need to remove the expected decaying aftershock
148 frequency from the time series. Nevertheless, the rate of aftershock decay 3-4 years after the
149 mainshocks is low, and the observation period in Figure 1 is only one month, and so the time
150 series in Figure 1 for at least box L appears convincing as long as post-Tohoku earthquakes
151 are not missing from the catalog.
152 Inconsistent with the static stress hypothesis, box D shows a delayed rate increase but no
153 stress increase, and there are seismicity rate increases in box A for which Coulomb stress
154 increases are present but do not dominate. Box B lacks sufficient focal mechanisms for

155 confident assessment. Box J, chosen to be centered on the Mj=6.7 shock, shows a rate
156 increase but a stress decrease. (Boxes N, O and P show little or no seismicity rate change or
157 stress change; they lie up to 600 km form the Tohoku rupture.) Box E is not analyzed because
158 the post-Tohoku seismicity is associated with shallow normal faulting, whereas the focal data
159 contain only deep reverse mechanisms.

160 A majority of the mechanisms along the Ou backbone mountain range (boxes B, C and D
161 in Figure 2b) are thought to be north-striking thrust faults, which would lie in the principal
162 stress shadow of the Tohoku mainshock, and thus be brought farther from failure [*Toda et al*.,
163 2011, submitted]. However, the significant percentage of strike-slip mechanisms and thrusts
164 of divergent strikes result in a large number of positive stress changes. This underscores that
165 resolving stress on the major faults alone idealizes the much more complex stress transfer.
166

167 **6. Discussion and Conclusions**

168 The fundamental observation driving this study is the widespread seismicity rate increase
169 across inland Japan, and extending to the Japan Sea and to the Izu island chain. Remarkably,
170 seismicity turned on at distances of up to 300 km from the lower edge of the Tohoku
171 earthquake rupture surface, and up to 425 km from the high (<15 m) slip zone. These
172 seismicity rate increases are apparent for M≥2 earthquakes, about half the boxes include M≥4
173 earthquakes and in four cases include M=5-6 earthquakes. Most of these increases follow the
174 Tohoku mainshock immediately, but some were delayed by up to several days. These distant
175 aftershocks could be triggered dynamically, they could be caused by the static stress changes,
176 or both. The maximum triggering distance, less than two source dimensions from the
177 mainshock, is consistent with the global absence M≥5 shocks triggered at greater distances
178 [*Parsons and Velasco*, 2011]. Here we explored the static hypothesis, which we adapted to the
179 special circumstances of triggering on very small faults that are neither optimally oriented in
180 the regional stress field nor parallel to the major faults. We thus use the Coulomb stress

181 change resolved on the nodal planes of the smallest earthquakes with focal mechanisms,
182 which limits us to M≥3.5 shocks, a ≥400 m rupture scale that at least overlaps that of the
183 aftershocks.

184 A tentative examination of the observed seismicity rate changes and calculated Coulomb
185 stress changes has met with promising but certainly incomplete success, since we find seven
186 positive three negative correlations (Table 1). Three of the positive correlations derive from
187 decreases both in observed seismicity rate and calculated Coulomb stress, and while we are
188 confident in the calculated stress decreases, it is perhaps too soon to be confident in the
189 seismicity rate declines.

190 Regardless of the process that promotes the aftershocks, we argue that the
191 microseismicity increases demonstrate that the 'remote' Japan Sea and inland Japan shocks
192 (e.g., Mw=6.3 on 3/12 03:59, Mw=6.2 on 3/12 04:46, Mw=5.8 on 3/15, 22:31) are neither
193 exceptional nor truly isolated events. Instead, they simply represent the largest shocks in a
194 very broad zone of elevated seismicity rate that is evident for M≥2 earthquakes.

195 One of the surprises of this work is that the effect of the stress shadow expected in
196 Tohoku for north-striking thrust fault appears—as yet—largely absent. Instead, much but not
197 all of Tohoku exhibits an increased rate of seismicity. Here we find that this behavior is
198 nevertheless consistent with static Coulomb stress transfer, but to smaller faults with
199 geometries different from the major faults, a possibility first advanced by *Marsan* [2006]. One
200 important question is whether the activation of these smaller divergent faults could trigger a
201 large event on one of the major thrusts, as might have occurred when the 15 June 1986
202 M~8-1/4 offshore Sanriku earthquake was succeeded by the 31 August 1896 Mj=7.2 Rikuu
203 inland earthquake at the same latitude (box B, Figure 2a). Since the 2011 Tohoku mainshock
204 is about ten times larger than the Meiji Sanriku mainshock, there could be large changes in
205 intraplate seismicity during the months to years ahead.
206

Acknowledgements. We thank David Hill and Andrea Llenos for thoughtful reviews, and we are grateful to JMA and NIED for the preliminary hypocenter list and focal mechanisms.

References

Churei, M. (2002), Relationships between eruptions of volcanoes, inland earthquakes (M≥6.2) and great tectonic earthquakes in and around north-eastern Japan Island arc, *J. Geography*, *111,* 175-184.

Grunewald, E., and R. S. Stein (2006), A new 1649-1884 catalog of destructive earthquakes near Tokyo and implications for the long-term seismic process, *J. Geophys. Res., 111*, doi:10.1029/2005JB004059.

Headquarters for Earthquake Research Promotion (2005), Report: 'National Seismic Hazard Maps for Japan (2005)', 162 pp, http://www.jishin.go.jp/main/index-e.html.

Hill, D. P. (2008), Dynamic stresses, Coulomb failure, and remote triggering, *Bull. Seismol. Soc. Amer.*, *98*, 66-92, doi:10.1785/0120070049.

King, G. C. P., R. S. Stein, and J. Lin (1994), Static stress changes and the triggering of earthquakes, *Bull. Seismol. Soc. Am*., *84*, 935-953.

Marsan, D. (2006), Can coseismic stress variability suppress seismicity shadows? Insights from a rate-and-state friction model *J. Geophys. Res. 111*, B06305, doi:06310.01029/ 02005JB004060.

McCloskey, J. Nalbant, S. S., S. Steacy, C. Nostro, O. Scotti, and D. Baumont (2003), Structural constraints on the spatial distribution of aftershocks, *Geophys. Res. Lett*., *30*, doi:10.1029/2003GL017225.

Nalbant, S. S., S. Steacy, K. Sieh, D. Natawidjaja, and J. McCloskey (2005), Earthquake risk on the Sunda trench, *Nature*, *435*, 756-757.

National Research Institute for Earth Science and Disaster Prevention (NIED), Broadband Seismograph Network (F-net), http://www.fnet.bosai.go.jp/top.php?LANG=en

Nyst, M., T. Nishimura, F. F. Pollitz, and W. Thatcher (2006), The 1923 Kanto earthquake re-evaluated using a newly augmented geodetic data set, *J. Geophys. Res.*, *111,* B11306, doi:11310.11029/12005JB003628.

Parsons, T., and A.A. Velasco (2011), Absence of remotely triggered large earthquakes beyond the mainshock region, *Nature Geoscience*, *4*, doi:10.1038/ngeo1110.

Pollitz, F. F., P. Banerjee, R. Burgmann, M. Hashimoto, and N. Choosakul (2006), Stress changes along the Sunda trench following the 26 December 2004 Sumatra-Andaman and 28 March 2005 Nias earthquakes, *Geophys. Res. Lett.*, *33*, L06309, doi:10.1029/2005GL024558.

Reasenberg, P. A., and R. W. Simpson (1992), Response of regional seismicity to the static stress change produced by the Loma Prieta earthquake, *Science*, *255*, 1687-1690.

Research Group for Active Faults in Japan, Active Faults in Japan (1991), sheet maps and inventories, rev. ed., 437 pp., Univ. Tokyo Press, Tokyo.

Seno, T. (1979), Intraplate seismicity in Tohoku and Hokkaido and large interplate earthquakes: A possibility of a large interplate earthquake off the southern Sanriku coast, northern Japan, *J. Phys. Earth*, *27*, 21-51.

Shimazaki, K. (1978), Correlation between intraplate seismicity and interpolate earthquakes in Tohoku, northeast Japan, *Bull. Seismol. Soc. Am.*, *68*, 181-192.

Toda, S., R. S. Stein, S. H. Kirby, and S. B. Bozkurt (2008), A slab fragment wedged under Tokyo and its tectonic and seismic implications, *Nature Geoscience*, *1*, 771-776, doi:10.1038.ngeo318.

Toda, S., J. Lin, R. S. Stein (2011), Using the 2011 M=9.0 Tohoku earthquake to test the Coulomb stress triggering hypothesis and to calculate faults brought closer to failure, submitted to *Earth, Planets and Space*.

Wells, D. L., and K. J. Coppersmith (1994), New empirical relationships among magnitude, rupture length, rupture width, rupture area, and surface displacement, *Bull. Seismol. Soc. Amer.*, *84*, 974-1002.

Wei, S. and A. Sladen, and the ARIA Group (2011), Updated result, 3/11/2011 (Mw 9.0), Tohoku-oki, Japan, http://tectonics.caltech.edu/slip_history/2011_taiheiyo-oki/index.html.

Table 1

Box Fig. 1	Min. Lon. (°)	Max. Lon. (°)	Min. Lat. (°)	Max. Lat. (°)	% positive ΔCFF *	Ave. ΔCFF (bar)	Seismicity Rate Change	Correlation between rate change and ΔCFF
A	138.80	139.40	40.10	40.70	27	-0.22	Increase	Negative
C	140.50	141.00	38.70	39.30	11	-3.3	Decrease	Positive
D	139.50	140.10	37.40	38.00	14	-1.3	Delayed increase	Negative
F	140.50	141.70	35.00	36.00	75	2.5	Increase	Positive
G	139.90	141.00	33.50	35.00	37	-0.04	Decrease	Positive
H	139.20	140.00	36.50	37.30	47	0.1	Increase	—
I	139.61	140.33	35.48	36.37	83	1.2	Increase	Positive
J	138.00	139.00	36.50	37.20	15	-0.4	Increase	Negative
K	137.20	137.80	35.95	36.80	88	0.3	Increase	Positive
L	136.20	137.00	37.00	37.50	19	-0.11	Decrease	Positive
M	138.80	139.50	34.00	35.70	82	0.1	Increase	Positive
N	138.90	139.70	41.20	43.00	59	0.05	No change	—
O	135.00	136.00	34.70	35.50	17	-0.04	No change	—
P	134.75	135.50	33.75	34.35	47	0	No change	—

* ΔCFF positive > 50% (red): <50% (blue). Ave. ΔCFF value > 0 (red); <0 (blue)

The percentage of nodal planes (two for each earthquake) with Coulomb stress increases and average stress change are compared with the observed seismicity rate change. Because of the preliminary state of the aftershock catalog, the correlations are approximate.

Figure Captions

Figure 1. (Left) Seismic response of inland Japan to the M=9.0 Tohoku mainshock. Map of the M≥1.0 seismicity rate change (27 day post-mainshock / 1.2 year pre-mainshock), with a smoothing radius of 20 km, using the JMA PDE catalog downloaded on 9 April 2011. Except for Box G (0-100 km), all boxes use 0-20 km depth. Dark green lines show plate boundaries. (Right) Time series show cumulative numbers of Mj≥0.0 earthquakes during 1/1–3/31/2011 (blue); each earthquake is shown as a green stem proportional to magnitude, M. The catalog is likely complete for M≥2.0.

Figure 2. Coulomb stress changes resolved on the nodal planes of small earthquakes as proxies for small active faults. (a) Focal mechanisms from the F-net catalog [*NIED*, 2011] since 1997 (depth ≤20 km for inland areas, ≤50 km for the eastern margin of Japan Sea region, and ≤100 km for Kanto); D is depth. (b) Maximum Coulomb stress change from each pair of nodal planes; where earthquakes overlap, the most positively-stressed shocks are plotted atop. The color of the box boundaries indicates the overall seismicity change inside each box: Increase (red), delayed increase (red dashed), decrease (blue), and no change (black).

Figure 3. Coulomb stress changes resolved on the nodal planes of the background earthquakes as proxies of local or regional fault structure in Chubu and Kinki districts. (a) Fault plane solutions since 1997 (depth ≤ 20 km). (b) Maximum Coulomb stress change from each pair of nodal planes.

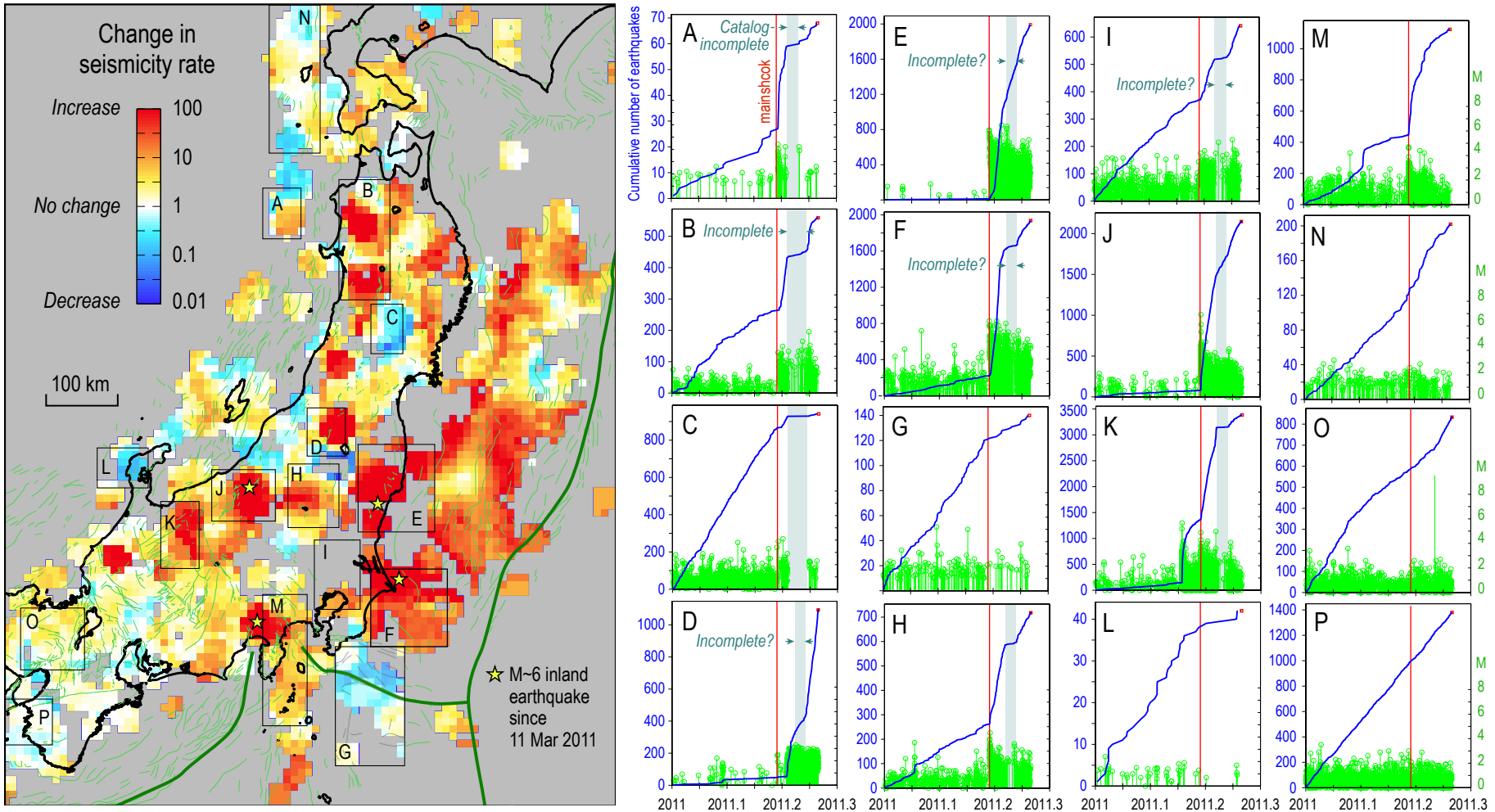
Change in seismicity rate
Increase
No change
Decrease
100
10
1
0.1
0.01
100 km
M~6 inland earthquake since 11 Mar 2011
Cumulative number of earthquakes
Catalog incomplete
mainshock
Incomplete
Incomplete?
2011
2011.1
2011.2
2011.3

Fig. 1

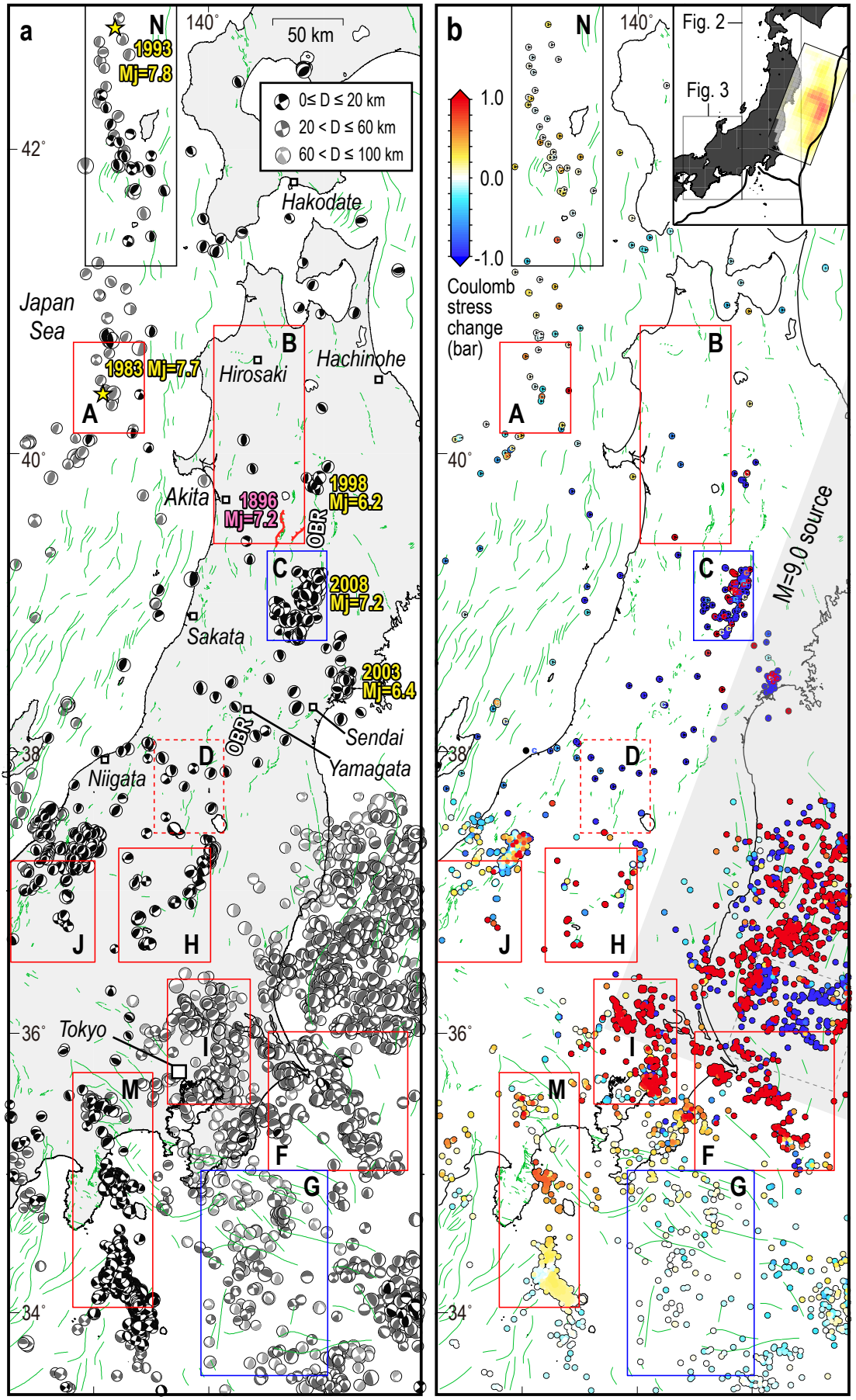
a
b
N
1993
Mj=7.8
140°
50 km
0≤ D ≤ 20 km
20 < D ≤ 60 km
60 < D ≤ 100 km
42°
Hakodate
Japan
Sea
1983 Mj=7.7
A
B
Hirosaki
Hachinohe
40°
Akita
1896
Mj=7.2
1998
Mj=6.2
OBR
C
2008
Mj=7.2
Sakata
2003
Mj=6.4
Sendai
Yamagata
38°
Niigata
D
OBR
J
H
36°
Tokyo
I
M
F
G
34°
1.0
0.0
-1.0
Coulomb
stress
change
(bar)
Fig. 2
Fig. 3
M=9.0 source

Fig. 2

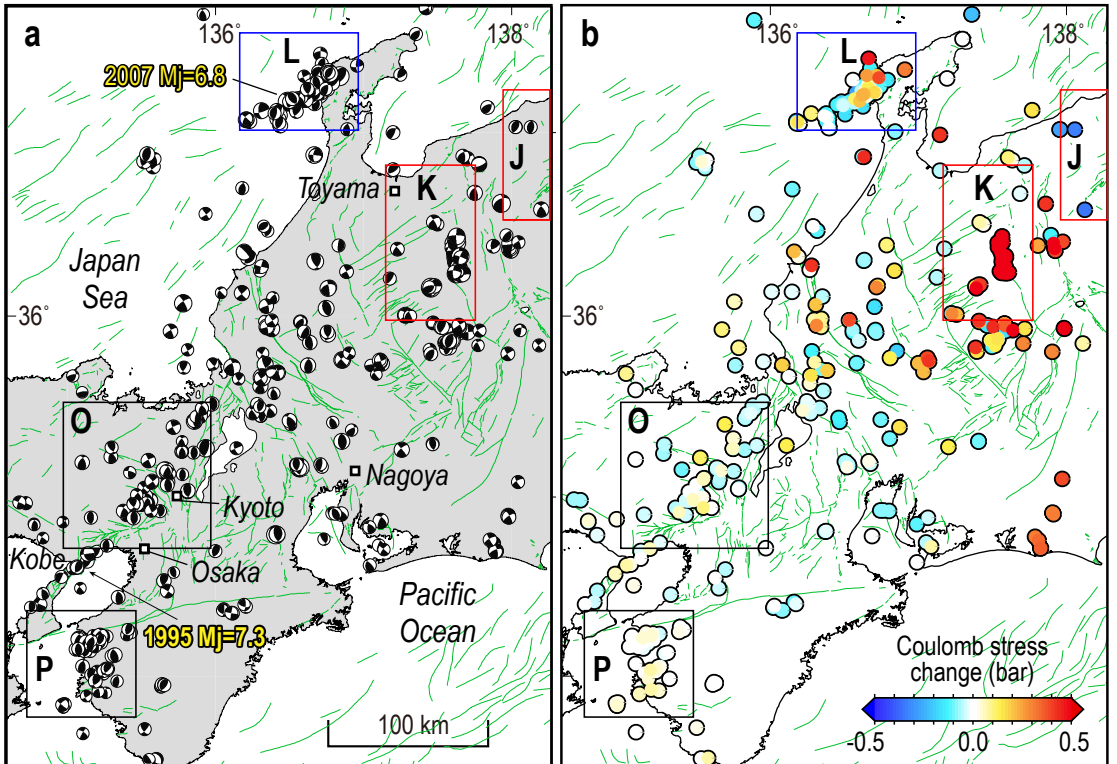
a
b
136°
138°
36°
L
J
K
O
P
2007 Mj=6.8
1995 Mj=7.3
Toyama
Japan
Sea
Nagoya
Kyoto
Kobe
Osaka
Pacific
Ocean
100 km
Coulomb stress
change (bar)
-0.5
0.0
0.5

Fig. 3